







Voronoi Cell Interface-Based Parameter Sensitivity Analysis for Labeled Samples - Supplemental Material

R. Bauer¹  M. Evers¹  Q. Q. Ngo¹  G. Reina¹  S. Frey²  and M. Sedlmair¹ 

¹Visualization Research Center (VISUS), University of Stuttgart, Germany

²University of Groningen, The Netherlands

Abstract

Varying the input parameters of simulations or experiments often leads to different classes of results. Parameter sensitivity analysis in this context includes estimating the sensitivity to the individual parameters, that is, to understand which parameters contribute most to changes in output classifications and for which parameter ranges these occur. We propose a novel visual parameter sensitivity analysis approach based on Voronoi cell interfaces between the sample points in the parameter space to tackle the problem. The Voronoi diagram of the sample points in the parameter space is first calculated. We then extract Voronoi cell interfaces which we use to quantify the sensitivity to parameters, considering the class label information of each sample's corresponding output. Multiple visual encodings are then utilized to represent the transitions and distributions, including stacked graphs for local parameter sensitivity. We evaluate the approach's expressiveness and usefulness with case studies for synthetic and real-world datasets.

CCS Concepts

• **Human-centered computing** → **Information visualization**; **Visual analytics**;

1. Plane-Plane-Metric

The plane-plane distance metric regarding the angle α between two (normal) vectors (see Figure 1) is shown in Figure 2.

2. Experimental Results on Runtimes and Bandwidth

The experiments were run on a consumer-grade laptop with 32GB RAM and Intel Core i7 – 10750H CPU. We varied the number of samples for a fixed dimensionality and bandwidth parameter in Fig-

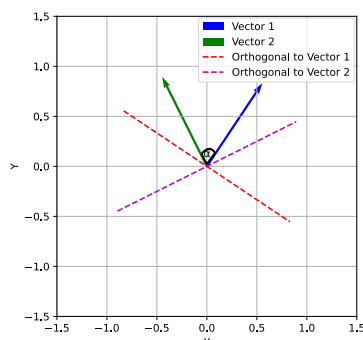


Figure 1: Two vectors with an angle α between each other.

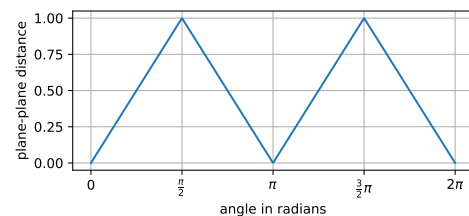


Figure 2: The plane-plane-distance metric given the angle (α) between two normalized vectors in radians.

ure 3. We varied the dimensionality for a fixed number of samples and bandwidth in Figure 4.

2.1. Variation of the Bandwidth for the Iris Dataset

In the normalized setting, i.e., all samples normalized to $[0, 1]$, the bandwidth $bw = \frac{1}{m}$, with m as the number of bins. We computed the label-to-label sensitivity using our approach of the Iris dataset for a variation of bandwidth parameters in terms of the number of bins. We report the corresponding runtimes in Figure 5. We report the corresponding visual encodings in Figure 6, Figure 7, Figure 8, Figure 9, Figure 10, Figure 11, Figure 12, Figure 13, Figure 14, Figure 15.

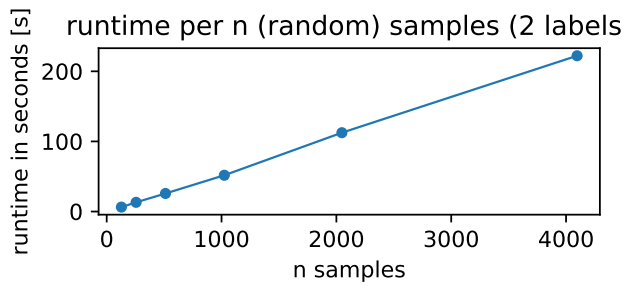


Figure 3: The running time per number of random samples in an artificial dataset ($\text{dim} = 4$, $m_{\text{bins}} = 10$). In our experiments, it appears to be growing linearly with the number of samples.

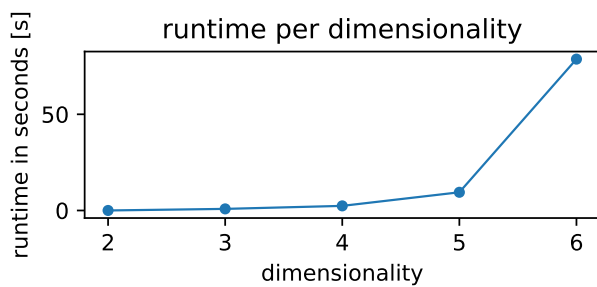


Figure 4: The running time per number of dimensions for an artificial dataset ($n_{\text{samples}} = 50$, $m_{\text{bins}} = 10$). In our experiments, it appears to be growing exponentially with the number of dimensions.

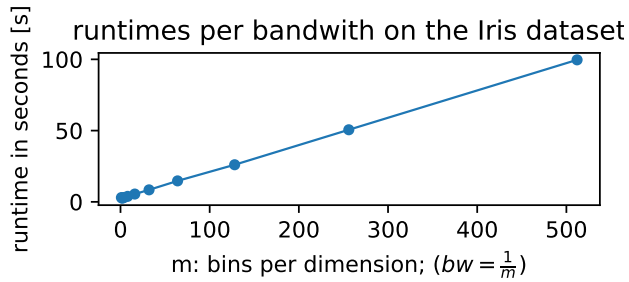


Figure 5: The running time per number of bins for the Iris dataset ($n_{\text{samples}} = 150$, $\text{dimensionality} = 4$). In our experiments, it appears to be growing linearly with the number of bins.

Acknowledgments

Funded by Deutsche Forschungsgemeinschaft (DFG, German Research Foundation) under Germany's Excellence Strategy - EXC 2075 - 390740016, Project 327154368 - SFB 1313 (D01), and Project 251654672 - TRR 161 (A01, A08). We acknowledge the support of the Stuttgart Center for Simulation Science (SimTech).

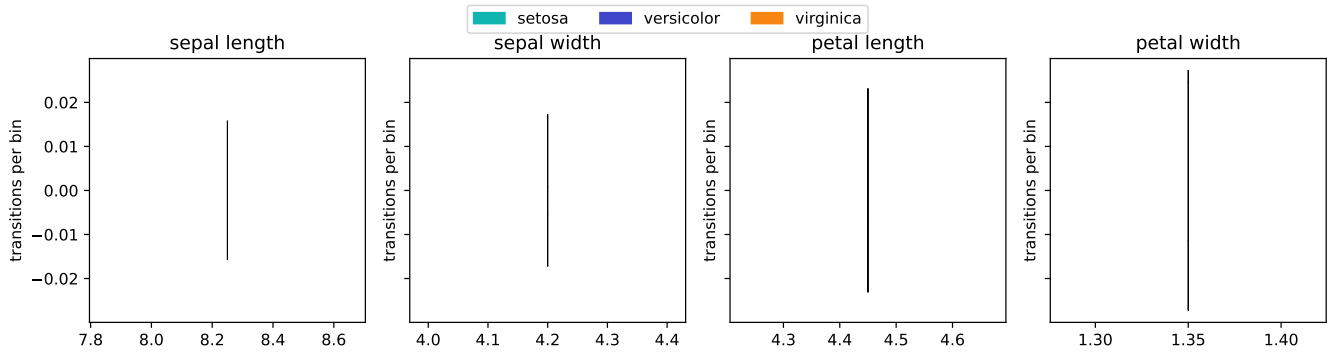


Figure 6: The label-to-label sensitivity utilizing our approach with 1 bin

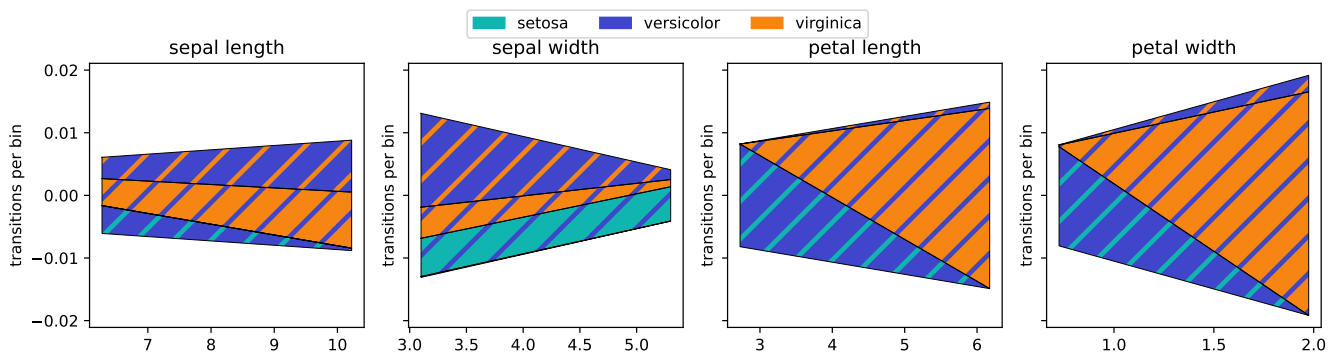


Figure 7: The label-to-label sensitivity utilizing our approach with 2 bins

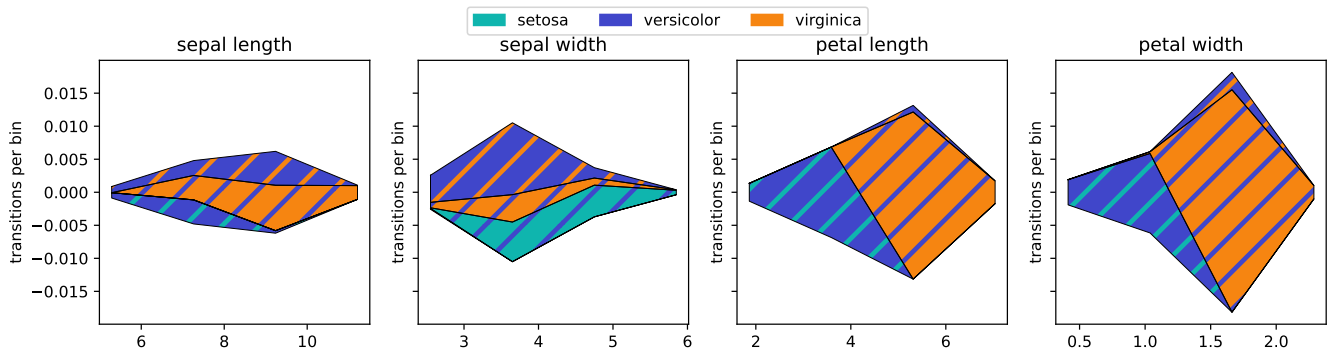


Figure 8: The label-to-label sensitivity utilizing our approach with 4 bins

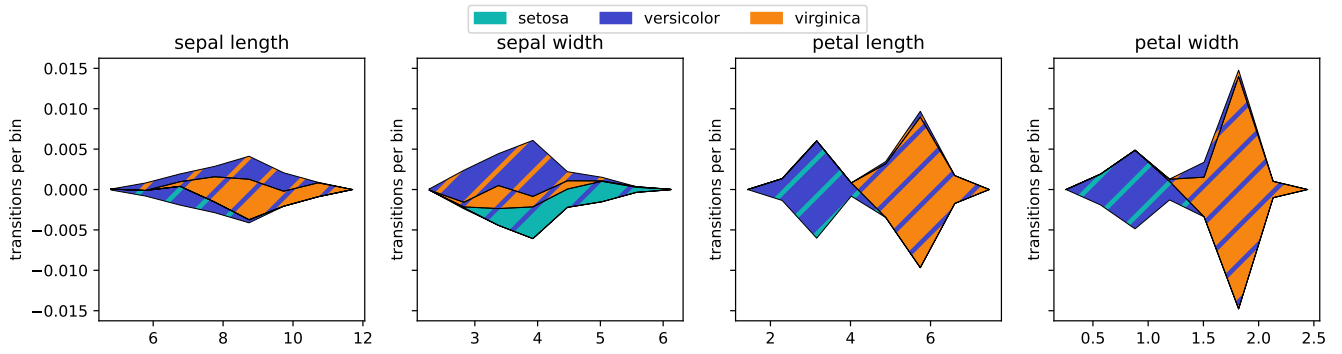


Figure 9: The label-to-label sensitivity utilizing our approach with 8 bins

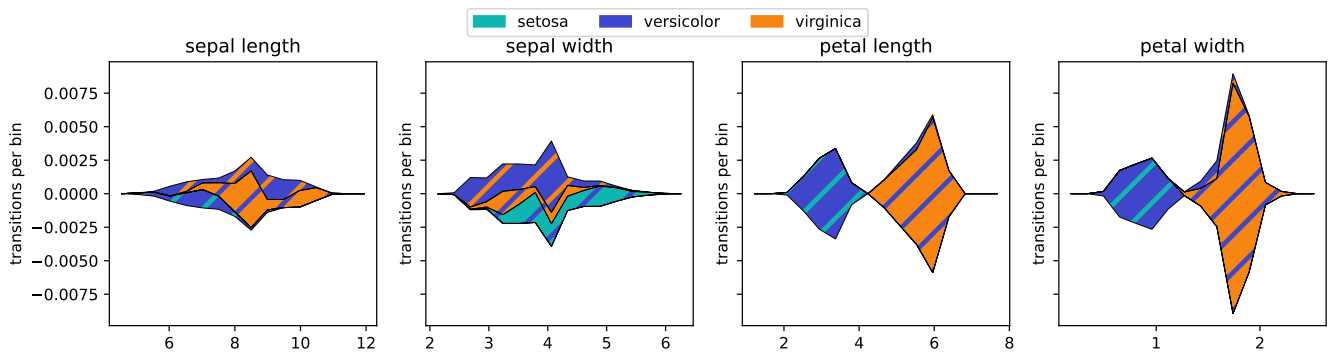


Figure 10: The label-to-label sensitivity utilizing our approach with 16 bins

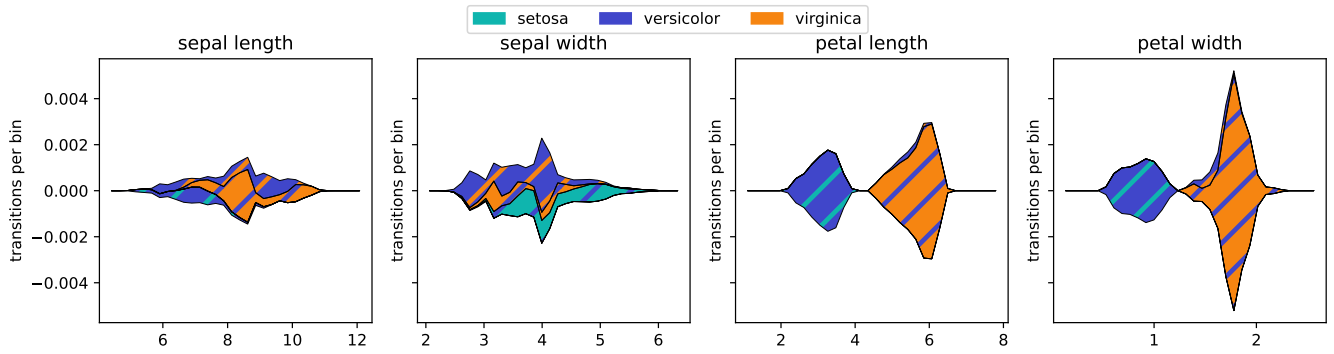


Figure 11: The label-to-label sensitivity utilizing our approach with 32 bins

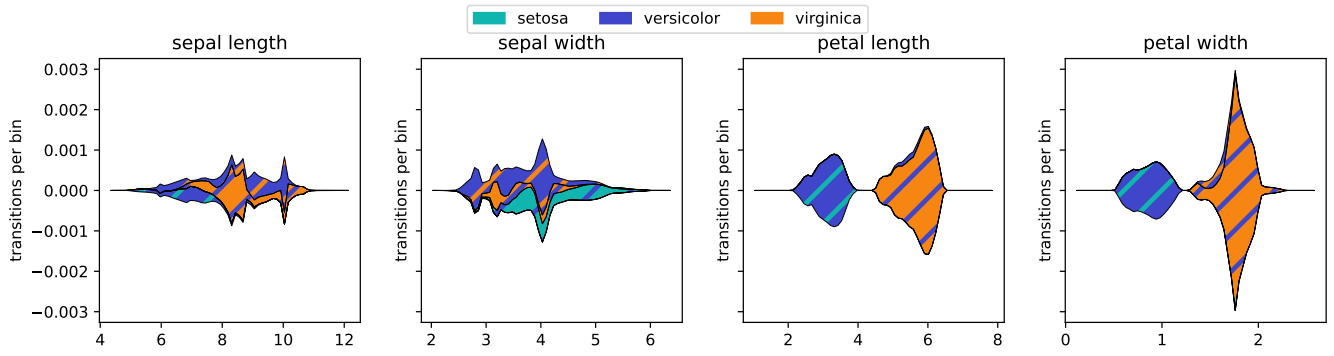


Figure 12: The label-to-label sensitivity utilizing our approach with 64 bins

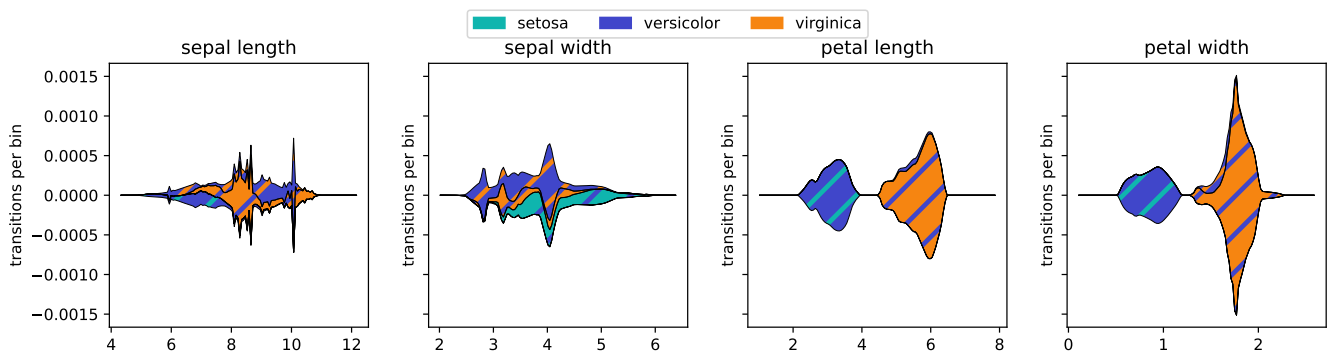


Figure 13: The label-to-label sensitivity utilizing our approach with 128 bins

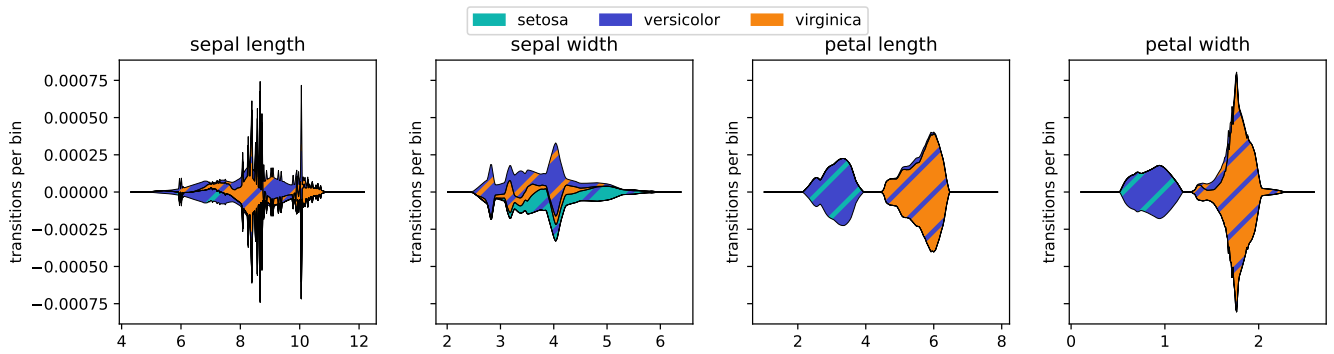


Figure 14: The label-to-label sensitivity utilizing our approach with 256 bins

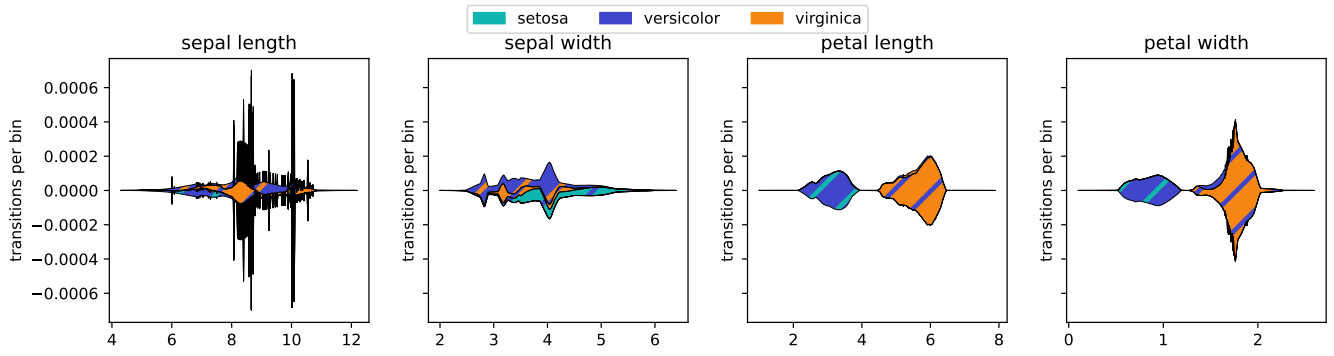


Figure 15: The label-to-label sensitivity utilizing our approach with 512 bins